2-2012

The Giant Danio (D. aequipinnatus) as a Model of Cardiac Remodeling and Regeneration

Pascal J. Lafontant
DePauw University, pascallafontant@depauw.edu

Jamie A. Grivas
DePauw University, jamiegrivas@depauw.edu

Mary A. Lesch
DePauw University

Lala Tanmoy Das
DePauw University, lalatanmoydas_2012@depauw.edu

Tyler D. Frounfelter
DePauw University

Recommended Citation

Lafontant, Pascal J., Alan R. Burns, Jamie A. Grivas, Mary A. Lesch, Tanmoy D. Lala, Sean P. Reuter, Loren J. Field, and Tyler D. Frounfelter, "The Giant Danio (D. aequipinnatus) as a Model of Cardiac Remodeling and Regeneration," *The Anatomical Record* 295, issue 2: 234-248. doi: 10.1002/ar.21492.

Published in final edited form as:
Anat Rec (Hoboken). 2012 February ; 295(2): 234–248. doi:10.1002/ar.21492.

The Giant Danio (D. aequipinnatus) as a Model of Cardiac Remodeling and Regeneration

Pascal J. Lafontant[1], **Alan R. Burns**[2,3], **Jamie A. Grivas**[1], **Mary A. Lesch**[1], **Tanmoy D. Lala**[1], **Sean P. Reuter**[4], **Loren J. Field**[4], and **Tyler D. Frounfelter**[1]

[1]DePauw University, Department of Biology, Greencastle, IN

[2]College of Optometry, University of Houston, Houston TX

[3]Department of Pediatrics, Baylor College of Medicine, Houston TX

[4]Wells Center for Pediatrics Research, Indiana University School of Medicine, Indianapolis, IN

Abstract

The paucity of mammalian adult cardiac myocytes (CM) proliferation following myocardial infarction (MI) and the remodeling of the necrotic tissue that ensues, result in non-regenerative repair. In contrast, zebrafish (ZF) can regenerate after an apical resection or cryoinjury of the heart. There is considerable interest in models where regeneration proceeds in the presence of necrotic tissue. We have developed and characterized a cautery injury model in the giant danio (GD), a species closely related to ZF, where necrotic tissue remains part of the ventricle, yet regeneration occurs. By light and transmission electron microscopy (TEM), we have documented four temporally overlapping processes: 1) a robust inflammatory response analogous to that observed in MI, 2) concomitant proliferation of epicardial cells leading to wound closure, 3) resorption of necrotic tissue and its replacement by granulation tissue, 4) regeneration of the myocardial tissue driven by 5-EDU and [^{3}H]thymidine incorporating CMs. In conclusion, our data suggest that the GD possesses robust repair mechanisms in the ventricle, and can serve as an important model of cardiac inflammation, remodeling and regeneration.

Keywords

Heart; Regeneration; giant danio; Remodeling; Zebrafish; Inflammation; cardiomyocytes

INTRODUCTION

The mechanisms of cardiac growth vary significantly within the life cycles of vertebrates (Rumyantsev, 1977). The interspecies differences that have been observed in mammalian and non-mammalian vertebrates are in part reflected in the varied ability of injured hearts to repair and regenerate (Borchardt and Braun, 2007; Ausoni and Sartore, 2009). During development, mammalian and non-mammalian hearts increase in size through two primary means: the differentiation of cardiomyogenic progenitor cells, and the proliferation of newly differentiated cardiac myocytes (hyperplasia) (Ahuja et al., 2007). Soon after birth, the preponderance of the evidence suggests that mammalian cardiac myocyte proliferation arrests following a quasi-irreversible exit out of the cell cycle (Brodsky et al., 1980; Soonpaa and Field, 1997). Indeed recent studies demonstrate that the neonatal mouse is able to regenerate its heart following resection only in the first week of life (Porrello et al., 2011).

Corresponding Author: Pascal J. Lafontant, 1 E Hanna st, Olin 258, DePauw University, Ph: (765) 658-4776, Fax: (765) 648-4766, pascallafontant@depauw.edu.

As a result, the archetypal response to injury observed in mammalian adult hearts consists of an effective but non-regenerative form of repair in which granulation tissue is progressively replaced with fibrotic tissue. Exceptions to this failure to regenerate are few, and have been reported in mouse models where cell cycle activation is maintained in adulthood (Chaudhry et al., 2004; Pasumarthi et al., 2005), and in models subjected to growth factors or to progenitor cell supplementation (Orlic et al., 2001; Beltrami et al., 2003; Urbanek et al., 2005; Ziebart et al., 2008). By contrast, many non-mammalian vertebrates remarkably retain the mechanisms that allow their cardiac myocytes to undergo hyperplasia, as demonstrated in the urodele amphibians such as the newt and axolotl (Neff et al., 1996; Bettencourt-Dias et al., 2003; Laube et al., 2006). As a result, significant regeneration in the heart of these species occurs following mechanical crushing injury (Laube et al., 2006) or partial ventricular amputation (Oberpriller and Oberpriller, 1974; Bader and Oberpriller, 1978; Bader and Oberpriller, 1979; Oberpriller et al., 1995; Flink, 2002; Vargas-Gonzalez et al., 2005).

In addition to amphibians, many fish species maintain the capacity for hyperplastic growth in adulthood (Clark and Rodnick, 1998); however regeneration of the fish heart has only been demonstrated in the zebrafish, *Danio rerio* (Poss et al., 2002; Raya et al., 2003). The use of the zebrafish as a model of heart regeneration has lead to the elucidation of several important signaling pathways and gene activities also present in mammalian systems during repair (Jopling et al., 2010; Kikuchi et al., 2010; Lepilina et al., 2006; Lien et al., 2006). Currently there is great interest in regeneration research to study closely related species, to determine their ability to generate different organs, in order to elucidate the evolution and the mechanisms of divergence in their regenerative capacities (Bely and Nyberg, 2010; Bely and Sikes, 2010). Within the cyprinids family, a closely related species to the zebrafish, the giant danio (GD) (Meyer et al., 1993) has been used as a model in a variety of studies. These include research in cone electrophysiology (Wong et al., 2005), retinal epithelium circuitry (Braekevelt, 1980; McMahon and Mattson, 1996; Wagner et al., 1998), histocompatibility (Graser et al., 1996), neurotrophic factor (Adams et al., 1996), swimming (Wolfgang et al., 1999), olfaction (Poling and Brunjes, 2000), vision (van Roessel et al., 1997). More recently the giant danio has been proposed as a model to study skeletal muscle growth (Biga and Goetz, 2006; Biga and Meyer, 2009). With a size twice as big as the zebrafish, as early as 4 weeks, the adult giant danio may be more amenable to surgical interventions and physiological studies. However whether the giant danio can regenerate its heart is not known.

In the zebrafish model, initiation of regeneration has been achieved through the amputation of the apical region of the myocardium in a manner that is analogous to studies performed in the urodele amphibians. More recently it was demonstrated that regeneration also occurs following cryoinjury (Chablais et al., 2011; Gonzalez-Rosa et al., 2011; Schnabel et al., 2011). In general, in mouse models of myocardial infarction, regeneration is not observed. The methods of injuries typically involve coronary ligation with and without reperfusion, and cauterization; these methods closely mimic the human insult, as the necrotic tissue remains part of the surviving myocardium and appears to influence the repair process (Rossen et al., 1985; Dreyer et al., 1992; Nossuli et al., 2001; Dewald et al., 2004). In these models the presence of the necrotic tissue leads to a robust inflammatory response that contributes to repair but leads to non-restorative remodeling, and the formation of a permanent scar (Frangogiannis et al., 2002; Frangogiannis, 2008). Although, recently the C57 mouse heart has been reported to regenerate following cryoinjury (van Amerongen et al., 2008), raising the question that injury methods in addition to species differences may determine the outcome of the reparative process. To date, the documentation of heart regeneration under varied experimental injuries is limited to relatively few vertebrate species (Table 1). In this study we wanted to determine whether the giant danio possesses the ability

to regenerate its heart and whether a cautery injury model that leaves significant necrotic tissue can lead to repair mechanisms that may model that observed in human cardiac infarction. We found that the temporally overlapping processes of inflammation, collagen accumulation and angiogenesis observed in mammalian models of infarction were accompanied by robust cell cycle re-entry in cardiac myocytes that lead to the regenerative reconstitution of the giant danio ventricle.

MATERIALS and METHODS

Animals

Giant danio 45 mm in standard length (SL, Table 2) were obtained from local provider, and maintain in 10-gallon tanks, with 15 to 20 fish per tank, at 28 degrees Celsius for two to three weeks prior to experiments, on 14/10 hours day/night cycles. Experimental procedures were approved by the Committee for the Care and Use of Laboratory Animals at DePauw University.

Surgery and ventricular cautery

On the day of the surgery, GD were removed from tanks and anesthetized with 0.02% MS Tricaine for one to two minutes and placed ventral side up in a slit cut in a wet rectangular-shaped sponge block. Using a Leica ZOOM 2000 dissecting microscope (Leica Microsystems, Bannockburn, IL) to guide the dissection, a pair of fine forceps was used to remove the scales above the thoracic cage; then the skin and the pectoral muscles were gently dissected midline, creating a 3 to 4 mm opening that revealed the silvery pericardial membrane. The pectoral muscles were kept retracted by one forceps while another forceps was used for the subsequent steps. The pericardial membrane was gently dissected to reveal the beating heart so that the apex could be identified. A Nichrome wire with a flat tip 0.455 mm diameter (24 gauge) was heated on an open flame Bunsen burner for 10 seconds, and left to cool for 3 seconds, then the tip of the wire was gently applied to the apex of the heart and left to cool an additional 3 to 5 seconds before removal from the apical surface. Following the cauterization procedure the fish were returned to a new freshwater tank. Fish were sacrificed at 1, 3, 7, 14, 21,30,45,60 and 180 days using 0.2% MS Tricaine. Once all body and opercula movements had ceased, the heart was removed by grasping and pulling the aorta proximal to the bulbus arteriosus. Heart weight, body weight and standard length were measured prior to further processing.

Measurements and characterization of injury by triphenyl tetrazolium chloride and Masson's trichrome

To assess the amount viable and non-viable tissue, triphenyl tetrazolium chloride (Sigma-Aldrich, Saint-Louis, MO) was prepared fresh in PBS and warmed to 28 degrees C. Tetrazolium chloride has been extensively used to assess area of necrosis in cardiac infarction models (Schaper and Schaper, 1983; Chi et al., 1989; Michael et al., 1995; Matsumura et al., 1998). The excised hearts were immediately transferred to 1.5-ml tubes containing 1 ml of 1% tetrazolium in PBS and incubated for 30 minutes, washed in PBS. They were photographed on one side projecting the largest cross-section perpendicular to the apex-bulbus axis, then tuned 180 degrees and photographed using a Nikon SMZ 1000 dissecting microscope (Nikon Instruments Inc., Melville, NY) equipped with a Spot Insight QE camera (Diagnostic Instruments Inc., Sterling heights, MI). Images were saved for later estimation of the injury size by morphometry. For measurement of viable and non-viable tissue images were projected on a Dell 17 inch monitor and overlaid with a 20 mm x 15 mm point-counting grid (20 × 14 point-intercepts) with 280 equidistant point-intercepts. Using the point-counting method the fraction of non-viable tissue was calculated based of the fraction of point intercepts landing randomly on the non-viable surface as indicated by the

white tissue to the total number of points lending on the red ventricular tissue. The measurements from the two images of the heart were averaged.

To assess area of injury in tissue sections, the hearts were removed and fixed in 4 % paraformaldehyde at 4 degrees C overnight. The next day the hearts were cryoprotected in 30% sucrose (Sigma-Aldrich, Saint Louis, MO), and placed in 13-mm diameter aluminum seal cups (Weathon, Millville, NJ), that were then filled with freezing medium (Tissue-tek OCT, Torrance, CA) and kept at −80 degrees prior to sectioning. The hearts were exhaustively sections sagittally on a Leica CM 1900 cryostat (Leica Microsystems, Bannockburn, IL). Following exhaustive serial sectioning, sections from the middle of each heart were stained and analyzed. Masson's trichrome staining was performed according to manufacturer's protocol (Sigma-Aldrich, Saint Louis, MO) with some modifications. Briefly, slides were rinsed in deionized water and incubated in preheated Bouin's solution at room temperature overnight. Slides were stained with acid hematoxylin solution for 5 minutes, and then washed in running tap water for 12 minutes. Next they were stained in 0.1% Biebrich Scarlet-0.1% Acid Fuchsin in 1% acetic acid for 5 minutes, and then incubated in 10% Phosphotungstic-Phosphomolybdic acid solution for 5 minutes, then in 2.4% Aniline Blue solution for 5 minutes, followed by 1% acetic acid. Slides were dehydrated through graded alcohol, cleared in xylene and mounted using Permount mounting medium (Electron Microscopy Sciences, Hatsfield, PA). Stained sections were visualized and imaged using a 4x objective on a Nikon Optiphot (Nikon Instruments Inc., Melville, NY) and the fraction of the injured area was measured using the point counting grid method.

Characterization of injury and regeneration in plastic section and by transmission electron microscopy

For studies of the myocardium in plastic sections and by transmission electron microcopy, the uninjured and injured hearts were fixed in 2.5 % fresh glutaraldehyde in 100mM cacodylate buffer overnight at 4 degrees C. The hearts were washed the next day in cacodylate buffer and stored at 4 degrees C for later processing. Hearts were post-fixed in 1% tannic acid and transferred to 1% osmium tetroxide, then were embedded in Embed-812 resin (Electron Microscopy Sciences, Hatsfield, PA) following dehydration in acetone. Two-micron sagittal sections were cut and toluidine-blue stained for light microscopy analysis. For electron microscopy analysis, ultra-thin sections 100 nm thick were cut, set on single slot or 200-mesh copper or nickel grids and imaged on a Tecnai G2 Spirit BioTWIN electron microscope (FEI Company, Hillsboro, OR).

Histochemical detection of inflammatory cells, endothelial cells, and collagen

Cryosections 10-microns thick were stained for the detection of inflammatory activity using Peroxidase (Myeloperoxidase) Leukocyte kit, according to the manufacturer's protocol (Sigma-Aldrich, Saint Louis, MO). Briefly, slides were washed in gently running tap water and allow to air dry in the dark. One vial of peroxidase indicator reagent and 200 μl of 3% hydrogen peroxide were added to 50 ml pre-warmed trizmal buffer. The slides were incubated in the peroxidase indicator reagent solution for 30 minutes in the dark at the 37 degrees C. Following incubation, the slides were washed in gently running tap water for 15–30 seconds and allowed to air dry. The slides were counterstained with Eosin, dehydrated in an alcohol-xylene series, air-dried and coverslipped using Permount. MPO positive cells were counted in two to three fields from 3 sections of each heart at 20x and averaged. For histochemical detection of endothelial cells, 10-micron sections were stained with FITC-labeled *Bandeiraea simplicifolia* lectin (Sigma-Aldrich) in Hepes buffer (10mM Hepes, 0.15M NaCl, 0.1M CaCl2, pH 7.5), overnight. Sections were washed the next day and cell nuclei where stained with Hoechst stain (Invitrogen, Eugene, OR) prior to visualization. For

collagen staining, sections from the middle of the heart were stained using Masson's Trichrome as described above. Each section was first imaged at 4x and the section area determined. For each section three fields were imaged in the area of the injury, and one field in an area remote from the injury, all at 40x. The fraction of blue stained fibers was calculated in the area on the injury and was later normalized to the entire section. The volume fraction excluded the luminal space of the ventricle.

Immunochemical detection of cell cycle progression and immunofluorescence detection of cardiac myocytes

For PCNA immunohistochemistry, hearts were fixed in ice cold 3.7% formaldehyde in ethanol (FA-ETOH), permeabilized with 0.5% triton X in PBS, and blocked with 3% BSA. PCNA antibody, PC10 clone (eBioscience, San Diego, CA) was used to incubate the sections at 4 degrees C, overnight. Biotinylated anti-mouse antibody was used as secondary antibody, followed by avidin-biotin complex and diaminobenzidine (Vectastain ABC kit, mouse IgG, and Peroxidase DAB substrate kit, Vector Laboratories, Burlingame, CA) according to the manufacturer's protocol. For myocyte enhancer factor (MEF) staining section were fixed in FA-ETOH and stained with MEF-2C (Santa Cruz Biotechnology Inc., Santa Cruz, CA) and an anti rabbit-FITC as a secondary antibody (Sigma-Aldrich). Sections were also stained with Hoechst and coverslipped using Permafluor mounting media (ThermoScientific, Freemont, CA).

Cell cycle activity by 5-ethynyl-2-deoxiuridine incorporation

In order to identify cells that have entered the cell cycle and progressed to S-phase in the heart, we studied the incorporation of 5-Ethynyl-2-deoxiuridine (EdU) using the Click-iT EdU kit (Invitrogen-Molecular Probes, Eugene, OR). EdU is a thymidine analog that is incorporated into DNA during S-phase transit. The Click-iT reaction allows the detection of the incorporated EdU using an azide-alkaline reaction and a fluorescent probe. EdU has been found to be as effective as BrdU in identifying cell cycle progression (Kaiser et al., 2009; Warren et al., 2009; Li et al., 2010). EdU was diluted in L-15 Leibovitz media without serum (Hyclone, Logan, UT). Each experimental and control heart was excised and transferred into 400 ul of EdU solution (50uM) in a 96 well plate pre-warmed at 28 degrees in an incubator. The hearts were returned to the incubator. After four hours the hearts were removed from the L-15 Leibovitz solution containing EdU, washed in PBS and fixed in FA-ETOH. EdU detection was performed following the manufacturer's protocol and was visualized with AlexaFluor 647. For double staining of EdU and myocyte enhancer factor (MEF), EdU detection was performed first, followed by MEF staining as described above.

Cardiac myocytes cell cycle re-entry by [^{3}H]thymidine incorporation and autoradiography

[^{3}H]Thymidine incorporation was performed ex-vivo in 96 well plates. Hearts were removed and incubated in 10 uCi [^{3}H]thymidine (20 Cu/mmol, Perkin-Elmer, Waltham, MA) in L-15 Leibovitz without serum for 4 hours. After 4 hours the hearts were washed in PBS and fixed in 2.5% glutaraldehyde in 100 nM cacodylate buffer, and embedded in plastic as described above. For autoradiography, 2 um unstained sections on slides were dipped for 10 seconds in Hypercoat emulsion (LM-1) melted at 43 degrees C (GE Life Sciences, Piscataway, NJ), in the dark room, under KODAK LED Safelight (Kodak, Rochester, NY). The slides were placed in light-proof boxes containing Dri-box reusable desiccant (Ted Pella, Redding, CA) and incubated in a refrigerator at 4 degrees C. After 4 days the slides were developed in Kodak D19 developer and fixed in ILFORD Rapid Fixer (Ilford, Avon, CT). Sections were dried and stained in 1% toluidine blue (Fisher Scientific, Hanover Park, IL) in 1% sodium borate and analyzed.

Statistical analysis

Data are means and +/−S.E.M. We used one way ANOVA followed by Student-Newman-Keuls post-test. Differences in which $p < 0.05$ were considered significant.

RESULTS

1. Characterization of cauterized giant danio heart by TTZ and Masson's trichrome staining

Cauterization of the giant danio heart produces a well defined injury occupying approximately 1/4th to 1/3rd of the ventricle (Fig. 1A, B), extending from the apex toward the base of the heart, and characterized grossly by the presence of a prominent central clot and bordering white pale tissue deprived of circulation. The surface area affected by the cauterization decreases over the first three weeks, with regression of the clot and reappearance of pink perfused tissue (Fig. 1C, D, E). By 45 days, the injured ventricle appeared grossly completely reconstituted (Fig. 1F). To determine the extent of tissue destruction caused by cauterization, sham and injured hearts were stained with TTZ. The non-viable tissue was identified by the whitish color indicating the tissue's inability to reduce the tetrazolium (Fig. 1G). The amount of viable myocardial tissue calculated at 97% in shams and at 72, 70 and 74% at 3 hours, 24 hours and 3 days respectively. By this measure, the amount of viable tissue returned to 96% by 60 days (Fig. 1H).

To estimate the extent of injury at the tissue level, 10 micron cryosections were stained using Masson trichrome in control and injured hearts up to 60 days. Similar to the zebrafish, the giant danio heart is comprised of thin compact myocardium that bordered the trabecular projections of the spongy myocardium in the control heart (Fig. 1I). In the injured heart, trichrome staining confirmed a complete loss of the compact heart architecture as well as the spongy trabecular projections in the injured area, a loss of luminal spaces between the trabeculae, replaced by clotting, and inhomogeneous interstitial material characteristic of necrosis (Fig. 1J). A distinct boundary was present between the injured and non-injured areas of the ventricle. In the remote non-injured area of the ventricle the architecture of the compact and spongy trabeculated heart was well preserved. The injured tissue area was comprised primarily of inhomogeneous connective tissue. The injured area was reduced by 14 days (Fig. 1K), concomitant with the appearance of a newly formed compact region, and partial reconstitution at the site of the inner wound. The myocardium appeared to be reconstituted by 60days, with the presence of a compact region as well as a spongy region of luminal space (Fig. 1L). However while the clear boundary between injured and non-injured area disappeared, small but quantifiable amount of connective tissue remained interspersed in the reconstituted myocardium. At 7 days the injured tissue area that occupied 27% of the myocardium was reduced at 45 days to 3% (Fig. 1M).

2. Injury characteristics by light microscopy of plastic sections and by EM

We further studied the characteristics of the cauterized region of the ventricle using 2 um toluidine blue stained plastic sections at 3, 7, and 14 days and by transmission electron microscopy 3 days after the injury. We found that the giant danio ventricle consists of a relatively thin compact layer penetrated by small vessels, and an extensive network of endocardial cell-lined trabeculae. At three days, the uninjured area of the ventricle showed a well defined compact heart and a dense meshwork of trabeculae filling the ventricular lumen. In the injured region, there was a complete loss of myocardial structure that encompassed the epicardium, and the compact and spongy myocardium in the apical injured region (Fig. 2A, arrow). A well defined border separated the injured and non- injured ventricular myocardium. TEM at 3 days revealed well organized actin-myosin filaments in the non-injured compact region and the trabeculae (Fig. 2B). The area of injury displayed myocardial necrosis in the compact and spongy regions, as well as numerous crenated and

necrotic nucleated red blood cells and inflammatory cells (Fig. 2C). We also observed fragmented cardiac myocytes with loss or disorganization of cellular content and actin-myosin filaments, as well as cardiac myocytes with mitochondrial cristae disruption at the injured border zone (Fig. 2D). At seven days the luminal injured area was filled with a mix of tissue and clot that did not display the phenotypic characteristics of cardiac myocytes (Fig. 2E), as compared to control (Fig. 2F). However a thin outer layer representing an epicardium could be observed (Fig 2E, arrows). By 14 days, a new compact myocardium lined with an epicardial cell layer was reconstituted. In addition myocardial trabeculae were projecting into the lumen of the ventricle towards the proximal border zone of the injury (Fig. 2G).

3. Inflammation

The presence and robustness of an inflammatory response impinges remarkably upon the repair and/or regeneration of mammalian and non-mammalian heart following injury to the ventricle. To determine whether an inflammatory response occurs following cauterization, its magnitude, and the time course of inflammatory cells infiltration, we studied myeloperoxidase (MPO) reactivity in 10 um cryosections of injured myocardium. Very few MPO positive cells (4 cells/field) could be observed in the compact region or the spongy region of the uninjured heart (Fig. 3A, E and L). However, 24 hours post-injury a marked presence of MPO positive cells (28 cells/field) could be found within the injured area and within the border zone (Fig. 3B, F and L). This number appears to decrease by 7 days (16 cells/field) but subsequently increase at 14 days (24 cells/field) and 21 days (24 cells/field) post-injury (Fig. 3C, G, and L). MPO positive cells decreased to the level of control hearts by 45 days (5 cells/field), (Fig. 3D, H, L). TEM revealed the presence of necrotic and viable inflammatory cells, consisting of heterophilic granulocytes at 3 days (Fig. 3I) in the cauterized myocardium and in the border zone between necrotic and viable tissue. Heterophilic granulocytes (Fig. 3J) and cells with monocytic and macrophage-like phenotypes (Fig. 3K) were also present at 14 days within the remaining granulation tissue and the regenerating myocardium.

4. Collagen deposition

The absence of collagen deposition or its accumulation leading to fibrosis is an important determinant of heart tissue repair or regeneration. To determine whether the regeneration of the injured area was accompanied with an accumulation of collagen, Masson's trichrome stained sections were analyzed in detail. Aniline blue stained fine fibrils indicating the presence of collagen could be identified in the inner face of the compact myocardium in uninjured ventricle, and accounted for 1.8% of the volume density of the apical region observed region (Fig. 4A, G, and H). At 7 days the volume density of collagen in the injured area was markedly increased to 20%, approximately 10 fold over control (Fig. 4B). The accumulation of collagen was further increased at 14 days (31%) and at 21 days (39%) in the regenerating compact and spongy region (Fig. 4 C, G, H). This accumulation decreased to 8% volume density by 60 days, however not to the level of non-injured hearts (Fig. 4D). Observations of regenerated hearts were extended to 180 days after injury when collagen fibril levels were comparable to that of control (data not shown). The presence of collagen fibrils was confirmed by TEM in the injured area at 14 days, and was found in between fibroblasts and inflammatory cells, in contact with fibroblasts and adjacent to small vessels (Fig. 4E, F). Collagen bundles were also observed in close proximity, but not in direct contact with cardiac myocytes.

5. Angiogenesis

To determine whether neovascularization accompanied the injury response, sections where stained with FITC-labeled *Bandeiraea simplicifolia* lectin. Lectin binding was readily

observed in a punctuate pattern along the apical arc of the compact myocardium, indicating the presence of small vessels, and in the endothelial cell layer lining the trabeculated myocardium (Fig. 5A, F, K). Lectin staining was lost 24 hours after cauterization in the area of the injury (Fig. 5B, G, L), but was still present in the region remote from the injury. At 14 days lectin staining was present in a diffuse pattern within the injured area indicating the presence of endothelial cells (Fig. 5C, H, and M). The lectin staining persisted at 21 days (Fig. 5D, I, N). At 45 days the punctate pattern of lectin positivity in small vessels in the regenerated compact myocardium and in the trabeculated region approximated that observed in the control heart (Fig. 5E, J, and O). The presence of small vessels in the compact myocardium was confirmed by TEM at 14 days. The vessels consisted of immature capillaries and small patent vessels with luminal RBC and leukocytic cells in the regenerated compact layer and in the regenerating spongy layer, interspersed between fibroblasts, myocytes and collagen bundles (Fig. 5P, Q).

6. Myocytes contribution to the regenerating myocardium

To determine the cellular basis of the regeneration in the cauterized giant danio heart, pulse labeling of hearts with EdU was performed ex vivo for 4 hours, 14 days following the excision of the heart from shams and injured giant danio. Pulse labeling with EdU and double staining with MEF antibody, a marker for myocytic cells, confirmed S-phase EdU incorporation in cells present in the regenerated compact and the regenerating trabeculated heart. A subset of EdU-positive cells that were also MEF-positive indicated that cardiac myocytes in the regenerating heart re-entered the cell cycle (Fig. 6A, B, and C). In parallel studies at 14 days, PCNA immunostaining revealed immunoreactivity in most of the cells in the reconstituted compact heart (Fig. 6D, E). PCNA immunoreactivity was also seen in the incompletely reconstituted trabeculated myocardium, while mostly absent in region distal to the injury (Fig. 6F).

To further confirm whether the cycling cells included cardiac myocytes, pulse labeling was performed ex vivo with [^{3}H]thymidine for 4 hours following the excision of hearts from shams and injured giant danio, and studied in 2 um toluidine-blue stained plastic sections following autoradiography. Very few [^{3}H]thymidine positive cells were found in epicardium, compact and trabeculated myocardium of sham animals. At 7 days however, a significant increase in [^{3}H]thymidine-positive cells were observed in the injured area, specifically in the outer single cell layer representing the epicardium (Fig. 6G, arrow) and within the granulation tissue occupied by non-myocytic cells (Fig. 6H, I). At 14 days [^{3}H]thymidine incorporation appeared in cells of the compact regions of the myocardium; while some of these cells were cardiac myocytes (Fig 6J, arrow) the types of many [^{3}H]thymidine-positive cells could not be easily determined. In the regenerating trabeculated region however (Fig. 6K, L, arrow), the cells observed incorporating [^{3}H]thymidine were primarily cardiac myocytes. Incorporation of [^{3}H]thymidine in cardiomyocytes in the trabeculated the myocardium showed a 10 fold increase compared to heart at time zero (Table 3). These observations indicated that cells incorporating [^{3}H]thymidine included cardiac myocytes and were contributing to the reconstitution of the injured area of the heart. Furthermore, TEM at 14 days revealed well differentiated cardiac myocytes in areas remote to the initial injury locus (Fig 7A). By contrast cardiac myocytes in the reconstituted compact and spongy heart at 14 days contained much less actin-myosin filaments and appears much less differentiated (Fig 7B).

DISCUSSION

In this study we have demonstrated that following cautery injury, the giant danio ventricular myocardium displays the spectrum of responses characteristic of a myocardial infarction: a robust and sustained infiltration of inflammatory cells, significant collagen accumulation,

and marked neovascularization. Cauterization results in a highly reproducible injury with resultant necrotic tissue. The injured area can be easily visualized in its gross aspect and estimated accurately upon removal using TTZ staining particularly in the earlier phase of the injury. Masson's trichrome staining of tissue sections provided histological evidence of the wound and for its estimation as well as evidence of the replacement of the wounded area with new myocardial tissue. The size and reproducibility of the injury is not unlike that achieved by resection of the apical area if the zebrafish ventricle (Poss et al., 2002). However unlike the resection model, in the cautery model the resulting wound and the necrotic tissue within which regeneration proceeds remain part of the heart and may influence the regenerative process. We speculate that the necrotic tissue might be in part responsible for the robust inflammatory response observed.

Inflammation is an important determinant of wound healing and repair in the heart (Frangogiannis et al., 2002; Dewald et al., 2004; Frangogiannis, 2008). Inflammation has been postulated as well to be an impediment to scarless healing and regeneration as pro-inflammatory cytokines released in the injury site can promote fibrogenic responses leading to scar formation. Support for this notion is provided by studies where absence or attenuation of inflammation results in scarless healing (Levesque et al., 2010;. Palatinus et al., 2010; Cowin et al., 1998; Wilgus et al., 2004). The zebrafish possesses a well developed innate immune system that includes granulocytes and macrophages (Lieschke et al., 2001) that are capable of mounting strong inflammatory responses (Neely et al., 2002; Phelps and Neely, 2005). Inflammation appears to be a cause for heart failure in zebrafish embryonic heart (Huang et al., 2007). Inflammatory gene induction has been documented as well in the regenerating zebrafish heart (Lien et al., 2006). While the cells comprising the innate immune system of the giant danio have not been previously characterized, we have demonstrated a robust inflammatory response in the cauterized heart and documented its subsequent resolution. Our findings suggest that the giant danio possesses a functional innate immune system that may be involved in injury and repair of the heart.

The finding of a double peak of inflammation was unexpected. Of note, a recent study in mouse cornea describes a double wave of neutrophils following abrasion (Li at al., 2006). The mechanisms underlying this pattern of neutrophil infiltration are not known. A second unexpected result consisted of the relatively prolonged inflammatory response compare to that observed in mammals. Indeed, in mammals the robust infiltration of granulocytes subsides quickly and is followed by a more temperate infiltration of monocytes and macrophages (Frangogiannis et al., 2002). Our MPO data do not distinguish between different types of inflammatory cells since MPO is also found in zebrafish heterophils and subsets of macrophages (Mathias et al., 2006; Brown et al., 2007; Mathias et al., 2009). Thus the two MPO-positive cells peaks may represent different cell populations. Indeed, at three days and later at two weeks, a variety of heterophilic and macrophage-like inflammatory cells are seen within the regenerating ventricle by TEM. The role of inflammation in this model and how it affects the course of regeneration will require further study.

Among the species with remarkable ability for heart regeneration, partial or complete, collagen accumulation has been reported but its magnitude has not been determined. It is generally agreed that the extent of collagen accumulation appears to be less significant than that observed in mammalian heart (Ausoni and Sartore, 2009). In contrast to mammals where large number of fibroblasts and circulating fibrocytes contribute to heart tissue (Haudek et al., 2010; Mollmann et al., 2006), zebrafish heart contains few resident fibroblasts, and they are primarily restricted to the subepicardial layer (Hu et al., 2000). In the zebrafish models, collagen accumulation appears to be transient. This underscores the possibility of a less robust capability of fibroblasts to produce collagen, the attenuation of

their activation or paucity of proliferation in the regenerating zebrafish heart. However it is important to note that zebrafish with a cell cycle checkpoint mutation (mps1) showed connective tissue scar formation during myocardial regeneration, suggesting that robust cardiac myocyte replacement might mitigate the accumulation of collagen (Poss et al., 2002).

In our model, collagen was significantly increased after the first week and was sustained in the weeks that followed. This increase was consistent with the observations of numerous fibroblasts and collagen fibers observed by TEM in the wound at 14 days. And while significantly decreased by 60 days, the resorption of accumulated collagen was only returned to non-injured level by 180 days suggesting that while permissive, the collagen accumulation was relatively refractory in comparison to the zebrafish. Whether this persistence in the giant danio heart is a function of the type of injury or a species specific response is unknown. Still the cautery injury and the resulting necrotic tissue may be analogous to a mammalian infarct and may provide a milieu in which fibroblasts can proliferate and for collagen to accumulate. We speculate that resorption of accumulated collagen in this model may require the orchestration of a robust remodeling program in which metalloproteinases (MMPs) and their inhibitors play a significant role. MMPs are upregulated in the regeneration of amputated zebrafish hearts (Kim et al., 2010; Lien et al., 2006). Moreover, the effective cardiac repair post myocardial infarction is dependent upon the balanced activity of these enzymes and their inhibitors: tissue inhibitor of MMPs (TIMPs) (Lindsey et al., 2003; Lindsey, 2004). Consequently, MMPs and TIMPs activity in the injured and regenerating giant danio heart warrants studies.

Regeneration in the presence of a strong inflammatory response and significant accumulation of collagen in our model is a compelling finding. This outcome might be in part dependent upon the extensive neovascularization observed within the wound. In mammals, the temporal evolution of collagen accumulation and neovascularization, as well as the balance of both processes are thought to differentially modulate and determine the outcome of heart repair. It is hypothesized that neovascularization may mitigate the development of fibrosis and promote potential mammalian cardiac myocytes proliferation (Dimmeler et al., 2005; Ziebart et al., 2008). Neovascularization has been reported in the zebrafish regenerating heart and is mediated by FGF1 (Lepilina et al., 2006) and PDGF (Kim et al., 2010). In our experiments both neovascularization and collagen accumulation are present at 7 and 14 days following the injury. TEM also reveals the presence of capillary structures throughout the wound at 14 days. These data suggest that neovascularization might balance if not mitigate the development of fibrosis, and may provide the permissive milieu for proliferating cardiac myocytes to regenerate the injured myocardium.

Data from this study suggest that regeneration occurs in three sequential but partially overlapping phases. First, the restoration of the epicardial layer takes place in the first week. Second, the compact heart is reconstituted during the second week. Third, the regeneration and maturation of the spongy heart is completed in the weeks that follow. Cell cycle activation in the epicardium very early after injury in the giant danio is similar to that observed in the zebrafish model where integrity of the epicardium is prioritized (Lepilina et al., 2006). Interestingly, cell cycle activity was pronounced in reconstituted compact layer during the second week. Outsprouting of myocytes from the compact myocardium could be seen projecting into the lumen of the ventricle, apical to basal, and to some extent lateral to medial, suggesting that regeneration may not proceed equally along the entire border zone. Interestingly, during embryonic development in zebrafish, the trabecular myocardium emerges from the compact myocardium by delamination or directed migration, (Liu et al., 2010). It appears that based on our observations the adult giant danio in part may

recapitulate this process. The regeneration of the new spongy heart may be primarily dependent on proliferating cardiac myocytes from the compact region.

The extent to which cardiac myocyte hyperplasia contributes to the regression of experimental infarct in adult mammalian models is still a matter of controversy. Less controversial is the role of adult cardiac myocyte hyperplasia in the regeneration of non-mammalian hearts, including the newt and axolotl. Various mechanisms have been proposed to explain the regeneration of the resected adult zebrafish heart. They range from the activation of progenitor cells from the epicardium to the cell cycle re-entry of dedifferentiated adult cardiac myocytes. The presence of less well differentiated cardiac myocytes in the regenerating region in our model is consistent with the two cited hypotheses. However, recent published studies supports the latter (Jopling et al., 2010; Kikuchi et al., 2010). Our study provides strong evidence that cardiac myocyte cell cycle re-entry contributes to the giant danio heart regeneration. However the lack of appropriate genetically modified giant danio with expression of cardiac-restricted markers, and the inconsistent and variable immunoreactivity of antibodies that we have thus far tested, precludes us from accurately estimating the exact magnitude of the contribution of cardiac myocyte hyperplasia to myocardial regeneration. We found however that [^{3}H]thymidine incorporation in thin plastic sections, particularly in the regenerating spongy heart, provided a reliable measure of spongy cardiac myocytes cell cycle activity. Our studies did not address whether progenitor cells contributes to regeneration. Yet, the mode by which the heart is regenerated suggests whether regeneration is supported by progenitor cells, dedifferentiating cardiac myocytes, or both, these cells may emerge first into the compact myocardium, before contributing to the emergent trabeculae.

In conclusion, our study demonstrates that heart regeneration in teleost fish is not restricted to the zebrafish. The cellular patterns of activity in many ways parallel those observed in models of mammalian myocardial infarction using coronary ligation. In our model the granulation tissue that included numerous vessels, inflammatory cells, fibroblasts, and collagen is progressively and effectively replaced by regenerated myocardium. We propose that cautery injury in the giant danio provides a reproducible and complementary model to study regenerative responses in fish, and the role of inflammation and permissive ventricular remodeling in heart regeneration.

Acknowledgments

Grant Sponsors: DePauw University’s Professional Development Funds. ARB Grant Sponsor: NIH; Grant #: EY017120, EY007551.

We thank Benjamin Golden and Amanda Miller for cryosectioning, Evelyn Brown for plastic sections and EM preparation, Margaret Gondo for EM technical support; Lynn Bedard, Henning Schneider, Chet Fornari and Tamara Beauboeuf for editorial suggestions, and the Biology Department Faculty for their support.

LITERATURE CITED

Abdullah I, Lepore JJ, et al. MRL mice fail to heal the heart in response to ischemia-reperfusion injury. Wound Repair Regen. 2005; 13(2):205–208. [PubMed: 15828946]

Adams DS, Kiyokawa M, Getman ME, Shashoua VE. Genes encoding giant danioand golden shiner ependymin. Neurochem Res. 1996; 21:377–384. [PubMed: 9139245]

Ahuja P, Sdek P, MacLellan WR. Cardiac myocyte cell cycle control in development, disease, and regeneration. Physiol Rev. 2007; 87:521–544. [PubMed: 17429040]

Ausoni S, Sartore S. From fish to amphibians to mammals: in search of novel strategies to optimize cardiac regeneration. J Cell Biol. 2009; 184:357–364. [PubMed: 19188493]

Bader D, Oberpriller J. Autoradiographic and electron microscopic studies of minced cardiac muscle regeneration in the adult newt, notophthalmus viridescens. JExp Zool. 1979; 208:177–193. [PubMed: 469482]

Bader D, Oberpriller JO. Repair and reorganization of minced cardiac muscle in the adult newt (Notophthalmus viridescens). J Morphol. 1978; 155:349–357. [PubMed: 633377]

Beltrami AP, Barlucchi L, Torella D, Baker M, Limana F, Chimenti S, Kasahara H, Rota M, Musso E, Urbanek K, Leri A, Kajstura J, Nadal-Ginard B, Anversa P. Adult cardiac stem cells are multipotent and support myocardial regeneration. Cell. 2003; 114:763–776. [PubMed: 14505575]

Bely AE, Nyberg KG. Evolution of animal regeneration: re-emergence of a field. Trends Ecol Evol. 2010; 25:161–170. [PubMed: 19800144]

Bely AE, Sikes JM. Latent regeneration abilities persist following recent evolutionary loss in asexual annelids. Proc Natl Acad Sci U S A. 2010; 107:1464–1469. [PubMed: 19966282]

Bettencourt-Dias M, Mittnacht S, Brockes JP. Heterogeneous proliferative potential in regenerative adult newt cardiomyocytes. J Cell Sci. 2003; 116:4001–4009. [PubMed: 12928330]

Biga PR, Goetz FW. Zebrafish and giant danio as models for muscle growth: determinate vs. indeterminate growth as determined by morphometric analysis. Am JPhysiol Regul Integr Comp Physiol. 2006; 291:R1327–1337. [PubMed: 16741137]

Biga PR, Meyer J. Growth hormone differentially regulates growth and growth-related gene expression in closely related fish species. Comp Biochem Physiol A Mol Integr Physiol. 2009; 154:465–473. [PubMed: 19654052]

Borchardt T, Braun T. Cardiovascular regeneration in non-mammalian model systems: what are the differences between newts and man? Thromb Haemost. 2007; 98:311–318. [PubMed: 17721612]

Braekevelt CR. Fine structure of the retinal epithelium and tapetum lucidum in the giant danio (danio malabaricus) (teleost). Anat Embryol (Berl). 1980; 158:317–328. [PubMed: 7356183]

Brodsky WY, Arefyeva AM, Uryvaeva IV. Mitotic polyploidization of mouse heart myocytes during the first postnatal week. Cell Tissue Res. 1980; 210:133–144. [PubMed: 7407859]

Brown SB, Tucker CS, Ford C, Lee Y, Dunbar DR, Mullins JJ. Class III antiarrhythmic methanesulfonanilides inhibit leukocyte recruitment in zebrafish. J Leukoc Biol. 2007; 82:79–84. [PubMed: 17431092]

Chablais F, Veit J, Rainer G, Jazwinska A. The zebrafish heart regenerates after cryoinjury-induced myocardialinfarction. BMC Dev Biol. 2011; 11:21. [PubMed: 21473762]

Chaudhry HW, Dashoush NH, Tang H, Zhang L, Wang X, Wu EX, Wolgemuth DJ. Cyclin A2 mediates cardiomyocyte mitosis in the postmitotic myocardium. J Biol Chem. 2004; 279:35858–35866. [PubMed: 15159393]

Chi LG, Tamura Y, Hoff PT, Macha M, Gallagher KP, Schork MA, Lucchesi BR. Effect of superoxide dismutase on myocardial infarct size in the canine heart after 6 hours of regional ischemia and reperfusion: a demonstration of myocardial salvage. Circ Res. 1989; 64:665–675. [PubMed: 2702730]

Clark RJ, Rodnick KJ. Morphometric and biochemical characteristics of ventricular hypertrophy in male rainbow trout (Oncorhynchus mykiss). J Exp Biol. 1998; 201:1541–1552. [PubMed: 9556537]

Cowin AJ, Brosnan MP, Holmes TM, Ferguson MW. Endogenous inflammatory response to dermal wound healing in thefetal and adult mouse. Dev Dyn. 1998; 212:385–393. [PubMed: 9671942]

Dewald O, Ren G, Duerr GD, Zoerlein M, Klemm C, Gersch C, Tincey S, Michael LH, Entman ML, Frangogiannis NG. Of mice and dogs: species-specific differences in the inflammatory response following myocardialinfarction. Am J Pathol. 2004; 164:665–677. [PubMed: 14742270]

Dimmeler S, Zeiher AM, Schneider MD. Unchain my heart: the scientific foundations of cardiac repair. J Clin Invest. 2005; 115:572–583. [PubMed: 15765139]

Dreyer WJ, Michael LH, Nguyen T, Smith CW, Anderson DC, Entman ML, Rossen RD. Kinetics of C5a release in cardiac lymph of dogs experiencing coronary artery ischemia-reperfusion injury. Circ Res. 1992; 71:1518–1524. [PubMed: 1423944]

Flink IL. Cell cycle reentry of ventricular and atrial cardiomyocytes and cells within the epicardium following amputation of the ventricular apex in the axolotl, Amblystoma mexicanum: confocal

microscopic immunofluorescent image analysis of bromodeoxyuridine-labeled nuclei. Anat Embryol (Berl). 2002; 205:235–244. [PubMed: 12107494]

Frangogiannis NG. The immune system and cardiac repair. Pharmacol Res. 2008; 58:88–111. [PubMed: 18620057]

Frangogiannis NG, Smith CW, Entman ML. The inflammatory response in myocardial infarction. Cardiovasc Res. 2002; 53:31–47. [PubMed: 11744011]

Gonzalez-Rosa JM, Martin V, Peralta M, Torres M, Mercader N. Extensive scar formation and regression during heart regeneration after cryoinjury in zebrafish. Development. 2011; 138:1663–1674. [PubMed: 21429987]

Graser R, O'HUigin C, Vincek V, Meyer A, Klein J. Trans-species polymorphism of class II Mhc loci in danio fishes. Immunogenetics. 1996; 44:36–48. [PubMed: 8613141]

Grisel P, Meinhardt A, et al. The MRL mouse repairs both cryogenic and ischemic myocardial infarcts with scar. Cardiovasc Pathol. 2008; 17:14–22. [PubMed: 18160056]

Haudek SB, Cheng J, Du J, Wang Y, Hermosillo-Rodriguez J, Trial J, Taffet GE, Entman ML. Monocytic fibroblast precursors mediate fibrosis in angiotensin-II-induced cardiac hypertrophy. J Mol Cell Cardiol. 2010; 49:499–507. [PubMed: 20488188]

Hu N, Sedmera D, Yost HJ, Clark EB. Structure and function of the developing zebrafish heart. Anat Rec. 2000; 260:148–157. [PubMed: 10993952]

Huang CC, Chen PC, Huang CW, Yu J. Aristolochic Acid induces heart failure in zebrafish embryos that is mediated by inflammation. Toxicol Sci. 2007; 100:486–494. [PubMed: 17823451]

Jopling C, Sleep E, Raya M, Marti M, Raya A, Belmonte JC. Zebrafish heart regeneration occurs by cardiomyocyte dedifferentiation and proliferation. Nature. 2010; 464:606–609. [PubMed: 20336145]

Kaiser CL, Kamien AJ, Shah PA, Chapman BJ, Cotanche DA. 5-Ethynyl-2′-deoxyuridine labeling detects proliferating cells in the regenerating avian cochlea. Laryngoscope. 2009; 119:1770–1775. [PubMed: 19554638]

Kikuchi K, Holdway JE, Werdich AA, Anderson RM, Fang Y, Egnaczyk GF, Evans T, Macrae CA, Stainier DY, Poss KD. Primary contribution to zebrafish heart regeneration by gata4(+) cardiomyocytes. Nature. 2010; 464:601–605. [PubMed: 20336144]

Kim J, Wu Q, Zhang Y, Wiens KM, Huang Y, Rubin N, Shimada H, Handin RI, Chao MY, Tuan TL, Starnes VA, Lien CL. PDGF signaling is required for epicardial function and blood vessel formation in regenerating zebrafish hearts. Proc Natl Acad Sci U S A. 2010; 107:17206–17210. [PubMed: 20858732]

Laube F, Heister M, Scholz C, Borchardt T, Braun T. Re-programming of newt cardiomyocytes is induced by tissue regeneration. J Cell Sci. 2006; 119:4719–4729. [PubMed: 17077121]

Leferovich JM, Bedelbaeva K, et al. Heart regeneration in adult MRL mice. Proc Natl Acad Sci U S A. 2001; 98:9830–9835. [PubMed: 11493713]

Lepilina A, Coon AN, Kikuchi K, Holdway JE, Roberts RW, Burns CG, Poss KD. A dynamic epicardial injury response supports progenitor cell activity during zebrafish heart regeneration. Cell. 2006; 127:607–619. [PubMed: 17081981]

Levesque M, Villiard E, Roy S. Skin wound healing in axolotls: a scarless process. J Exp Zool B Mol Dev Evol. 2010; 314:684–697. [PubMed: 20718005]

Li K, Lee LA, Lu X, Wang Q. Fluorogenic "click" reaction for labeling and detection of DNA in proliferating cells. Biotechniques. 2010; 49:525–527. [PubMed: 20615206]

Li Z, Burns AR, Smith CW. Two waves of neutrophil emigration in response to corneal epithelial abrasion: distinct adhesion molecule requirements. Invest Ophthalmol Vis Sci. 2006; 47:1947–55. [PubMed: 16639002]

Lien CL, Schebesta M, Makino S, Weber GJ, Keating MT. Gene expression analysis of zebrafish heart regeneration. PLoS Biol. 2006; 4:e260. [PubMed: 16869712]

Lieschke GJ, Oates AC, Crowhurst MO, Ward AC, Layton JE. Morphologic and functional characterization of granulocytes and macrophages in embryonic and adult zebrafish. Blood. 2001; 98:3087–3096. [PubMed: 11698295]

Lindsey ML. MMP induction and inhibition in myocardial infarction. Heart Fail Rev. 2004; 9:7–19. [PubMed: 14739764]

Lindsey ML, Mann DL, Entman ML, Spinale FG. Extracellular matrix remodeling following myocardial injury. Ann Med. 2003; 35:316–326. [PubMed: 12952018]

Liu J, Bressan M, Hassel D, Huisken J, Staudt D, Kikuchi K, Poss KD, Mikawa T, Stainier DY. A dual role for ErbB2 signaling in cardiac trabeculation. Development. 2010; 137:3867–3875. [PubMed: 20978078]

Mathias JR, Dodd ME, Walters KB, Yoo SK, Ranheim EA, Huttenlocher A. Characterization of zebrafish larval inflammatory macrophages. Dev Comp Immunol. 2009; 33:1212–1217. [PubMed: 19619578]

Mathias JR, Perrin BJ, Liu TX, Kanki J, Look AT, Huttenlocher A. Resolution of inflammation by retrograde chemotaxis of neutrophils in transgenic zebrafish. J Leukoc Biol. 2006; 80:1281–1288. [PubMed: 16963624]

Matsumura K, Jeremy RW, Schaper J, Becker LC. Progression of myocardial necrosis during reperfusion of ischemic myocardium. Circulation. 1998; 97:795–804. [PubMed: 9498544]

McMahon DG, Mattson MP. Horizontal cell electrical coupling in the giant danio: synaptic modulation by dopamine and synaptic maintenance by calcium. Brain Res. 1996; 718:89–96. [PubMed: 8773769]

Meyer A, Biermann CH, Orti G. The phylogenetic position of the zebrafish (Danio rerio), a model system in developmental biology: an invitation to the comparative method. Proc Biol Sci. 1993; 252:231–236. [PubMed: 8394584]

Michael LH, Entman ML, Hartley CJ, Youker KA, Zhu J, Hall SR, Hawkins HK, Berens K, Ballantyne CM. Myocardial ischemia and reperfusion: a murine model. Am J Physiol. 1995; 269:H2147–2154. [PubMed: 8594926]

Mollmann H, Nef HM, Kostin S, von Kalle C, Pilz I, Weber M, Schaper J, Hamm CW, Elsasser A. Bone marrow-derived cells contribute to infarct remodelling. Cardiovasc Res. 2006; 71:661–671. [PubMed: 16854401]

Neely MN, Pfeifer JD, Caparon M. Streptococcus-zebrafish model of bacterial pathogenesis. Infect Immun. 2002; 70:3904–3914. [PubMed: 12065534]

Neff AW, Dent AE, Armstrong JB. Heart development and regeneration in urodeles. Int J Dev Biol. 1996; 40:719–725. [PubMed: 8877445]

Nossuli TO, Frangogiannis NG, Knuefermann P, Lakshminarayanan V, Dewald O, Evans AJ, Peschon J, Mann DL, Michael LH, Entman ML. Brief murine myocardial I/R induces chemokines in a TNF-alpha-independent manner: role of oxygen radicals. Am J Physiol Heart Circ Physiol. 2001; 281:H2549–2558. [PubMed: 11709422]

Oberpriller JO, Oberpriller JC. Response of the adult newt ventricle to injury. J Exp Zool. 1974; 187:249–253. [PubMed: 4813417]

Oberpriller JO, Oberpriller JC, Matz DG, Soonpaa MH. Stimulation of proliferative events in the adult amphibian cardiac myocyte. Ann N Y Acad Sci. 1995; 752:30–46. [PubMed: 7755274]

Oh YS, Thomson LE, et al. Scar formation after ischemic myocardial injury in MRL mice. Cardiovasc Pathol. 2004; 13:203–206. [PubMed: 15210135]

Orlic D, Kajstura J, Chimenti S, Limana F, Jakoniuk I, Quaini F, Nadal-Ginard B, Bodine DM, Leri A, Anversa P. Mobilized bone marrow cells repair the infarcted heart, improving function and survival. Proc Natl Acad Sci U S A. 2001; 98:10344–10349. [PubMed: 11504914]

Palatinus JA, Rhett JM, Gourdie RG. Translational lessons from scarless healing of cutaneous wounds and regenerative repair of the myocardium. J Mol Cell Cardiol. 2010; 48:550–557. [PubMed: 19560469]

Pasumarthi KB, Nakajima H, Nakajima HO, Soonpaa MH, Field LJ. Targeted expression of cyclinD2 results in cardiomyocyte DNA synthesis and infarct regression in transgenic mice. Circ Res. 2005; 96:110–118. [PubMed: 15576649]

Phelps HA, Neely MN. Evolution of the zebrafish model: from development to immunity and infectious disease. Zebrafish. 2005; 2:87–103. [PubMed: 18248169]

Poling KR, Brunjes PC. Sensory deafferentation and olfactory bulb morphology in the zebrafish and related species. Brain Res. 2000; 856:135–141. [PubMed: 10677620]

Porrello ER, Mahmoud AI, Simpson E, Hill JA, Richardson JA, Olson EN, Sadek HA. Transient regenerative potential of the neonatal mouse heart. Science. 2011; 331:1078–1080. [PubMed: 21350179]

Poss KD, Wilson LG, Keating MT. Heart regeneration in zebrafish. Science. 2002; 298:2188–2190. [PubMed: 12481136]

Raya A, Koth CM, Buscher D, Kawakami Y, Itoh T, Raya RM, Sternik G, Tsai HJ, Rodriguez-Esteban C, Izpisua-Belmonte JC. Activation of Notch signaling pathway precedes heart regeneration in zebrafish. Proc Natl Acad Sci U S A. 2003; 100(Suppl 1):11889–11895. [PubMed: 12909711]

Robey TE, Murry CE. Absence of regeneration in the MRL/MpJ mouse heart following infarction or cryoinjury. Cardiovasc Pathol. 2008; 17:6–13. [PubMed: 18160055]

Rossen RD, Swain JL, Michael LH, Weakley S, Giannini E, Entman ML. Selective accumulation of the first component of complement and leukocytes in ischemic canine heart muscle. A possible initiator of an extra myocardial mechanism of ischemic injury. Circ Res. 1985; 57:119–130. [PubMed: 3874008]

Rumyantsev PP. Interrelations of the proliferation and differentiation processes during cardiact myogenesis and regeneration. Int Rev Cytol. 1977; 51:186–273. [PubMed: 338537]

Schaper J, Schaper W. Reperfusion of ischemic myocardium: ultrastructural and histochemical aspects. J Am Coll Cardiol. 1983; 1:1037–1046. [PubMed: 6833643]

Schnabel K, Wu CC, Kurth T, Weidinger G. Regeneration of cryoinjury induced necrotic heart lesions in zebrafish is associated with epicardial activation and cardiomyocyte proliferation. PLoS One. 2011; 6:e18503. [PubMed: 21533269]

Soonpaa MH, Field LJ. Assessment of cardiomyocyte DNA synthesis in normal and injured adult mouse hearts. Am J Physiol. 1997; 272:H220–226. [PubMed: 9038941]

Urbanek K, Torella D, Sheikh F, De Angelis A, Nurzynska D, Silvestri F, Beltrami CA, Bussani R, Beltrami AP, Quaini F, Bolli R, Leri A, Kajstura J, Anversa P. Myocardial regeneration by activation of multipotent cardiac stem cells in ischemic heart failure. Proc Natl Acad Sci U S A. 2005; 102:8692–8697. [PubMed: 15932947]

van Amerongen MJ, Harmsen MC, Petersen AH, Popa ER, van Luyn MJ. Cryoinjury: a model of myocardial regeneration. Cardiovasc Pathol. 2008; 17:23–31. [PubMed: 18160057]

van Roessel P, Palacios AG, Goldsmith TH. Activity of long-wavelength cones under scotopic conditions in the cyprinid fish Danio aequipinnatus. J Comp Physiol A. 1997; 181:493–500. [PubMed: 9373956]

Vargas-Gonzalez A, Prado-Zayago E, Leon-Olea M, Guarner-Lans V, Cano-Martinez A. Myocardial regeneration in Ambystoma mexicanum after surgical injury. Arch Cardiol Mex. 2005; 75(Suppl 3):S3-21–29. [PubMed: 16366167]

Wagner TL, Beyer EC, McMahon DG. Cloning and functional expression of a novel gap junction channel from the retina of Danio aquipinnatus. Vis Neurosci. 1998; 15:1137–1144. [PubMed: 9839978]

Warren M, Puskarczyk K, Chapman SC. Chick embryo proliferation studies using EdU labeling. Dev Dyn. 2009; 238:944–949. [PubMed: 19253396]

Wilgus TA, Bergdall VK, Tober KL, Hill KJ, Mitra S, Flavahan NA, Oberyszyn TM. The impact of cyclooxygenase-2 mediated inflammation on scarless fetal wound healing. Am J Pathol. 2004; 165:753–761. [PubMed: 15331400]

Wolfgang MJ, Anderson JM, Grosenbaugh MA, Yue DK, Triantafyllou MS. Near-body flow dynamics in swimming fish. J Exp Biol. 1999; 202:2303–2327. [PubMed: 10441083]

Wong KY, Adolph AR, Dowling JE. Retinal bipolar cell input mechanisms in giant danio. I. Electroretinographic analysis. J Neurophysiol. 2005; 93:84–93. [PubMed: 15229213]

Ziebart T, Yoon CH, Trepels T, Wietelmann A, Braun T, Kiessling F, Stein S, Grez M, Ihling C, Muhly-Reinholz M, Carmona G, Urbich C, Zeiher AM, Dimmeler S. Sustained persistence of transplanted proangiogenic cells contributes to neovascularization andcardiac function after ischemia. Circ Res. 2008; 103:1327–1334. [PubMed: 18927463]

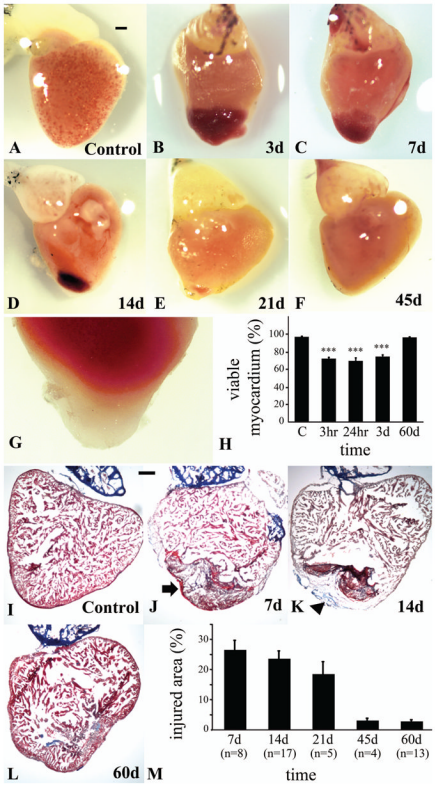

Figure 1.

Regeneration of GD ventricle following cautery injury. Gross morphology of GD heart observed on a dissecting microscope of (A) control ventricle, and (B) cauterized ventricle at day 3 with a clearly visible clot (b). (C) Regression of the clot at day 7, (D) day 14, (E) day 21, (F) day 45 after the injury. (G) TTZ stained ventricle showing non-viable tissue in apical portion of the ventricle at 24 hr. (H) Estimation of the volume of ventricle occupied by non-viable tissue from day one to day 60 after the injury. Representative Masson's trichrome stained sagittal sections of (I) control heart, (J) 7 day heart illustrating the presence of a clot and concomitant loss of myocytic tissue in the injured area (arrow), and (K) the progressive reconstitution of myocardial structure (arrowhead) at 14 days and (L) 60 days. (M) Quantification of the size of the injured area with its component connective tissue as they are replaced by of the myocardial tissue. (Scale bars, 200 um)

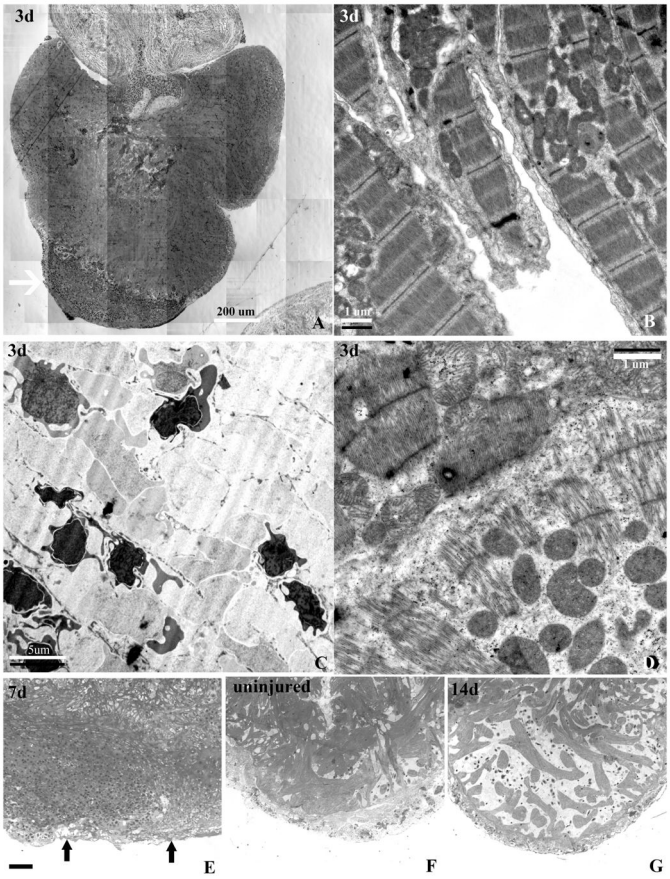

Figure 2.

Characterization of the injury induced by cauterization in plastic sections and by transmission electron microscopy. (A) Montage of a toluidine blue stained 2-um plastic-embedded section of an injured GD ventricle at day 3 post-injury demonstrating a well defined area of injury with loss of myocytes (arrow). (B) Transmission electron micrograph of well organized trabeculated myocytes with well organized sarcomeres, Z-bands, and dense area of mitochondria in a region distal from the injury. (C) Ultrastructure within the injured area showing complete loss of myocyte structure and the presence of crenated nucleated red blood cells contributing to the clot. (D) Ultrastructure of myocytes at the border zone of the injury showing disorganized and lower density of sarcomere closer to the injured area (lower half oh panel), and myocytes with higher sarcomeric density and organization (upper half of panel). (E) Toluidine blue stained section of a heart 7 days after the injury showing a loss of the structural characteristics of the compact and spongy heart showing, and (F) an uninjured heart with well defined compact and the dense trabeculated spongy myocardium. (G) Reconstitution of the compact heart is coupled with the reappearance of a spongy heart of lesser trabecular density at 14 days.

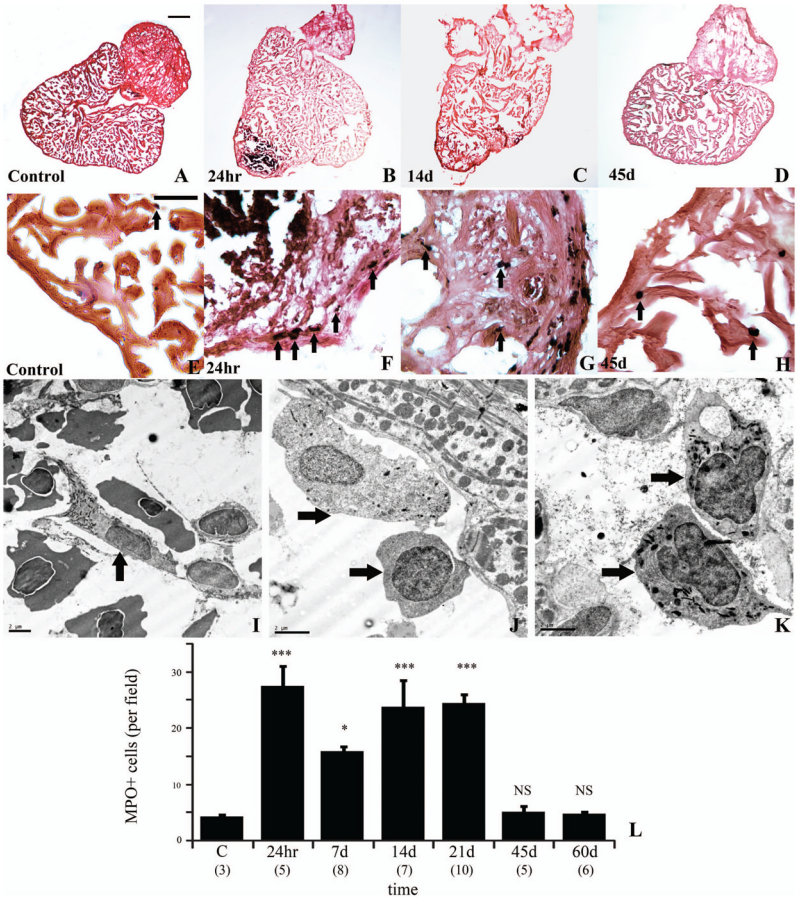

Figure 3.

Inflammation in the injured and regenerating GD heart. Myeloperoxidase immune reactivity (black, arrow) in control heart (A, E higher magnification) section counterstained with eosin (orange). Marked presence of immunoreactive cells at 24 hr (B, F higher magnification), 14 days (C, G higher magnification), decreasing at 45 days (D, H higher magnification). Representative TEM of an heterophilic granulocyte (I, arrow) with cigar-shaped granule at 3 days, and an heterophilic granulocyte (J, top arrow), monocyte (J, bottom arrow), and macrophages (K, arrows) at 14 days in injured area. (L) Kinetics of MPO-positive cells infiltrating the injured GD heart. (Scale bar A–D, 200 um; scale bar E–H, 50 um, scale bar TEM, 2 um)

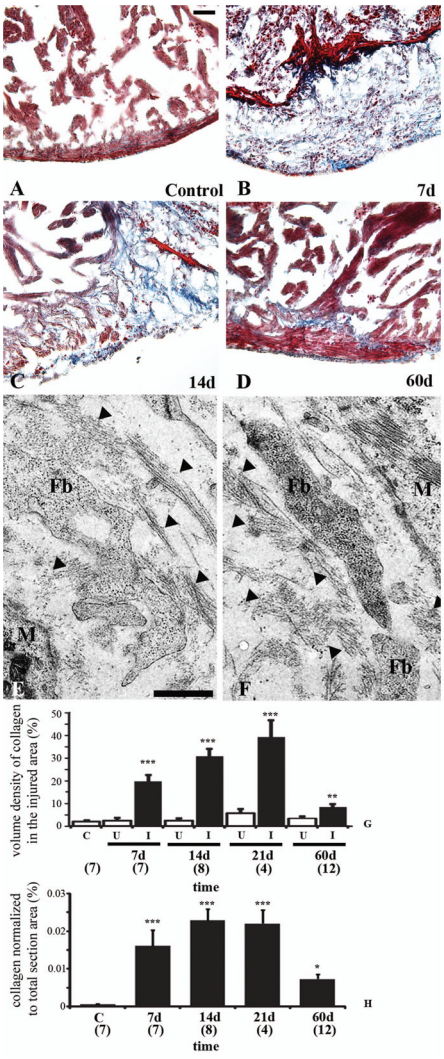

Figure 4.

Collagen accumulation and resorption during GD ventricular remodeling following cauterization. (A) Trichrome stained heart of GD showing minimal presence of collagen (blue fibrils) in the non-injured heart. Accumulation of collagen increases at (B) 7 days, (C) 14 days, and decreases (D) at 45 days. (E, F) Collagen fibril bundles (arrowheads) running in multiple directions adjacent to fibroblasts (Fb) and myocytes (M) within injured GD ventricle at 14 days. (G) Quantification of aniline blue stained collagen fibrils in trichrome stained section in injured and non-injured areas, and (H) in injured area normalized to ventricular area. (Scale bar A–D, 50 um; scale bar E–F, 1 um)

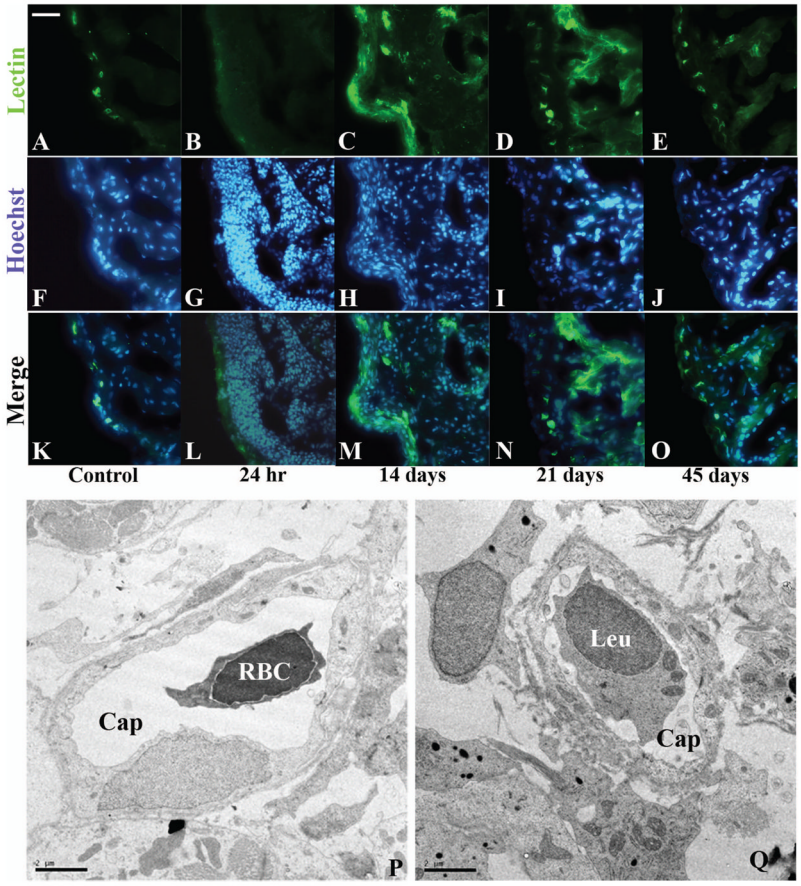

Figure 5.

Angiogenic response in the cauterized GD ventricle. (A) B.S. lectin-FITC staining in control heart outlines small vessels in the compact heart. Staining is absent (B) 24 hours following injury but is present in diffused clusters within the wound at 14 days (C). Scattered lectin staining persists at (D) 21 days within the wound, and is regressed to outline the regenerated endocardium and small vessels of the regenerated compact heart at 45 days (E). Hoechst staining of cell nuclei in the control section (F), show increase cell nuclei at (G) 24 hours, (H) 14days, (I) 21 days, and returning to control level at (J) 45 days. (K, L, M, N, O) overlay of A and F, B and G, C and H, D and I, E and J. (P) Representative TEM of a small capillary-like vessel (Cap) with a circulating red blood cell (RBC) in the wound at 14 days, and (Q) another vessel (Cap) with a circulating leukocyte (Leu). (Scale bar A–O, 50 um, scale bar TEM, 2 um)

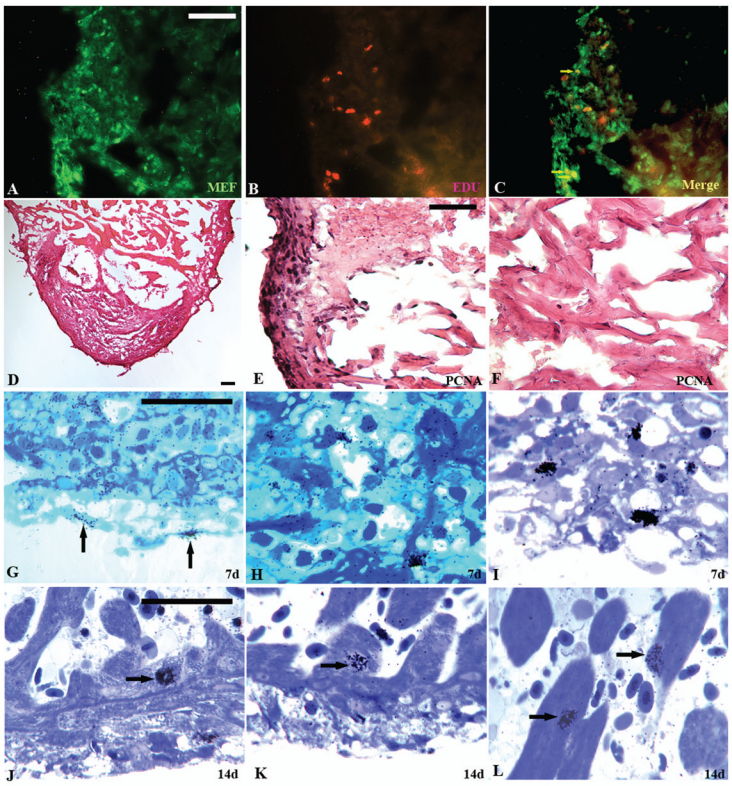

Figure 6.

Epicardial cells and cardiac myocytes support GD heart regeneration. MEF immunoreactivity (A) and EdU incorporating cells (B) in the regenerating area at 14 days, and overlay of MEF and EdU incorporation showing numerous MEF+/EdU+ cells (C, arrow) indicating cardiac myocyte cell cycle activation. Immunoreactivity of PCNA in regenerating GD heart section (D) counterstained with eosin at 14 days. Higher magnification image of the compact myocardium (E) showing marked PCNA immunoreactivity, and original spongy area bordering the proximal part of the injury (F) with few PCNA immunoreactive cells. [^{3}H]Thymidine incorporation (silver grains) in toluidine blue stained section at 7 days showing epicardial cell cycle activation (G, arrow), and cells in the evolving connective tissue (H, I). [^{3}H]Thymidine incorporation in cells of the regenerated compact heart (J, K, arrow) and the regenerating spongy heart cardiac myocytes (L, arrow) at 14 days. (Scale bars, 50 um).

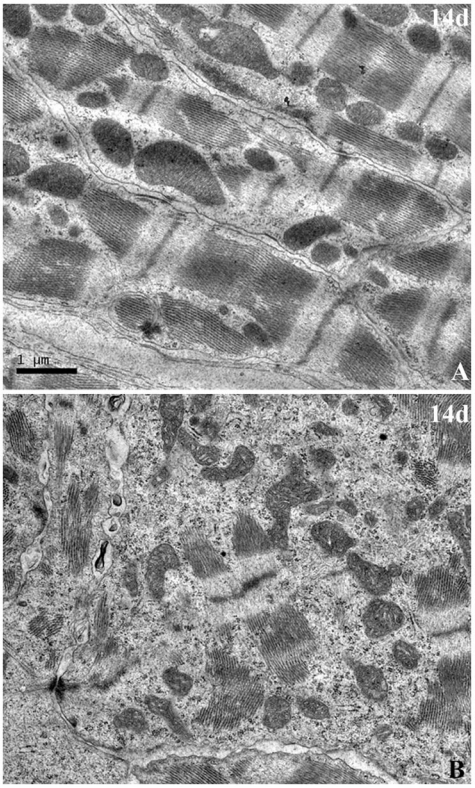

Figure 7.
Cardiac myocytes ultrastructure in regenerating myocardium. (A), TEM of myocardium in area remote from the site of injury at 14 days with myocytes containing well organized and aligned sarcomeres, and well ordered Z bands. (B), TEM of myocardium in the injured and regenerating are containing myocytes with less well orgazined sarcomeric components and few Z-bands (Scale bar, 1um for A and B).

Table 1

Heart Regeneration Studies in Vertebrates.

Models	Injury Method	Regeneration	References
Mouse			
• Neonatal	Resection	Yes	(Porrello, Mahmoud et al. 2011)
• MRL, adult	cryoinjury	Yes	(Leferovich, Bedelbaeva et al. 2001)
	coronary ligation or cryoinjury	No	(Oh, Thomson et al. 2004; Abdullah, Lepore et al. 2005; Grisel, Meinhardt et al. 2008; Robey and Murry 2008)
•Adult	Cryoinjury, C57BL	Yes	(van Amerongen, Harmsen et al. 2008)
• Adult	Cryoinjury, C57BL	No	(Grisel, Meinhardt et al. 2008; Robey and Murry 2008)
Amphibians			
• Adult Newt (N. viridecens)	Resection, Mechanical crush	Yes	(Oberpriller and Oberpriller 1974; Bader and Oberpriller 1978}
• Axolotl (A. mexicanum)	Resection	Yes	(Flink 2002; Vargas-Gonzalez, Prado-Zayago et al. 2005)
• Newt	Mechanical crush	Yes	(Laube, Heister et al. 2006)
Teleost fish	Resection	Yes	(Poss, Wilson et al. 2002; Raya, Koth et al. 2003)
• Zebra fish	Cryoinjury	Yes	(Chablais, Veit et al. 2011; Gonzalez Rosa, Martin et al. 2011; Schnabel, Wu et al. 2011)

Table 2

Heart Weight (HW), standard lenght (SL), and body weight (BW) in control and experimental giant danio.

time	**0** ***n = 23***	**7d** ***n =28***	**14d** ***n =55***	**21d** ***n = 11***	**45d** ***n = 14***	**60d** ***n =21***	**180d** ***n = 7***
HW (mg)	2.6+/−1.9	3.1+/−0.2	3.2+/−0.1	3.2+/1− 0.2	3.1+/−0.3	3.0+/−0.2	3.1+/−0.3
SL (mm)	46.4+/−1.1	45.9+/− 0.9	47.3+/− 0.9	47.6+/− 1.4	47.1+/−1.0	48.7+/−0.8	50.6+/− 1.7
BW(g)	1.6+/−0.1	1.6+/−0.1	1.8+/−0.1	1.7+/−0.1	1.7+/−0.1	2.1+/−0.1	2.1+/−0.1
HW/SL(*100)	5.5+/−0.4	6.8+/−0.4	6.6+/−0.2	6.6+/−0.3	6.1+/−0.5	6.6+0.4	6.3+/−1.0
HW/BW(*100)	167.7+/−10.7	202.5+/−8.8	183.8+/−6.0	191.14+/−7.4	177.6+/−1.6	142.5+/−9.8	150.0+/−16.3

Data are means +/− SEM.

Table 3

Cardiomyocyte cell cycle progression in regenerating spongy myocardium.

	Thymidine + cardiomyocytes count	number of fields	Thymidine + cardiomyocytes per field
control, n = 4	1	32	0.022+/−0.022
14 days, n = 7	23	63	0.365+/−0.102 *

* p<0.05 compared to control. Cardiomyocytes/field data are means+/− SEM